Supporting Information

What Can Probing Liquid-Air Menisci Inside Nanopores Teach Us About Macroscopic Wetting Phenomena?

Binyu Zhao,[†,‡] Youquan Jia,[†] Yi Xu,[†] Elmar Bonaccurso,[⊥] Xu Deng,[‖] Günter K. Auernhammer,[‡,§] and Longquan Chen*[,†]

[†] School of Physics, University of Electronic Science and Technology of China, Chengdu 610054, China

[‡] Leibniz Institute of Polymer Research Dresden, Dresden 01069, Germany

[⊥] Airbus Central R&T, Materials X, Munich 81663, Germany

[‖] Institute of Fundamental and Frontier Sciences, University of Electronic Science and Technology of China, Chengdu 610054, China

[§] Max Planck Institute for Polymer Research, Ackermannweg 10, Mainz 55128, Germany

* **Corresponding author**. E-mail: lqchen@uestc.edu.cn

Contents

Table S1. Geometric dimensions and wetting properties of the flat alumina and diverse nanoporous AAO surfaces. D, S, H are the diameter, interpore distance and height of pores, respectively. θ_{adv} is the advancing contact angle, θ_{rec} is the receding contact angle and their difference $\Delta\theta = \theta_{adv} - \theta_{rec}$ is the contact angle hysteresis.

D/nm	0	57±5	83±7	232±36	321±28	362±29	552±55	599±57	653±84
S/nm	-	98±6	124±8	424±39	454±49	465±52	942±110	1004±73	1023±104
H/μm	-					5±1			
θ_{app}/°	100±2	134±3	145±1	148±5	149±3	151±1	151±1	150±4	150±3
θ_{adv}/°	110±2	143±2	153±5	153±2	154±1	155±1	155±1	155±2	155±1
θ_{rec}/°	90±1	56±2	104±1	144±2	148±4	149±3	149±3	151±1	150±1
$\Delta\theta$/°	20±2	87±3	48±5	9±1	6±3	6±2	6±3	4±2	6±2

Table S2. The roughness factor (r_W), the solid fraction (f_S), and the fractions of the liquid-solid (f_{SL}) and liquid-air (f_{LA}) interfacial areas of diverse nonwetting nanoporous surfaces.

D/nm	57±5	83±7	232±36	321±28	362±29	552±55	599±57	653±84
r_W	97±14	69±12	33±8	32±8	24±6	13±4	13±3	12±3
f_S	0.53±0.01	0.42±0.01	0.60±0.01	0.39±0.02	0.35±0.01	0.58±0.01	0.61±0.01	0.57±0.01
f_{LS}	1.13±0.06	0.73±0.06	1.20±0.09	0.68±0.11	0.32±0.03	1.34±0.09	0.89±0.07	0.77±0.05
f_{LA}	0.53±0.02	0.65±0.02	0.39±0.04	0.60±0.07	0.81±0.03	0.36±0.03	0.55±0.04	0.68±0.03

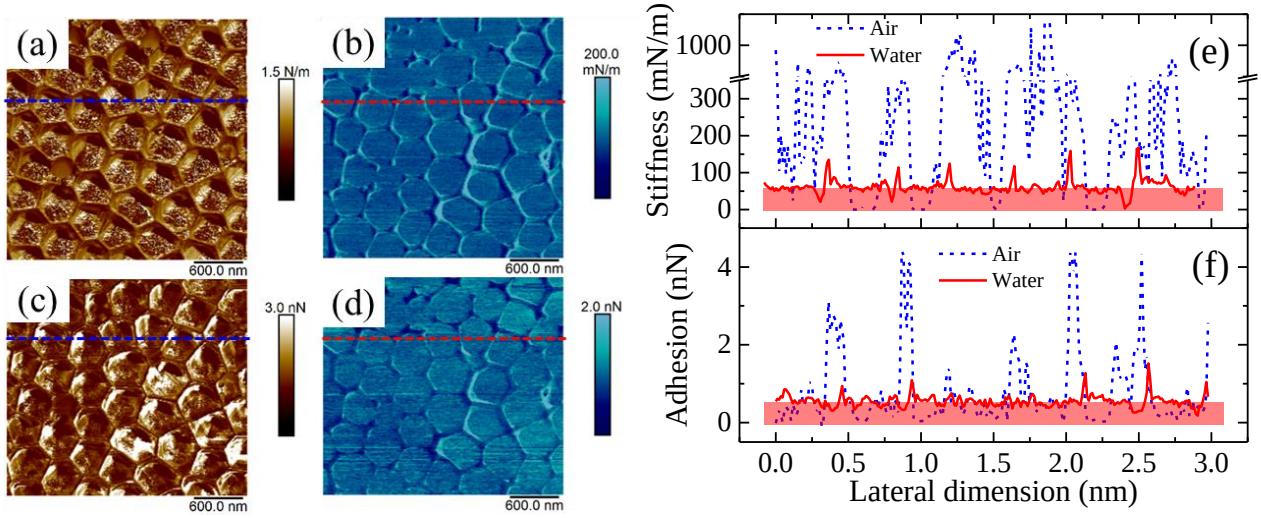

Figure S1. Nanomechanical maps on a nonwetting nanoporous surface. **(a-d)** *In situ* AFM stiffness (**a**, **b**) and (**c**, **d**) adhesion images of the nanoporous surface with $D \approx 362\,nm$ in air (**a**, **c**) and beneath a water droplet (**b**, **d**). (**e**, **f**) The corresponding cross-section profiles along the indicated scanning lines. Note that the stiffness and adhesion profiles [blue dashed lines in (**e**) and (**f**), respectively] on solid areas do not reflect the real stiffness and adhesion values because the employed soft cantilevers are not suitable for characterizing the rigid alumina.

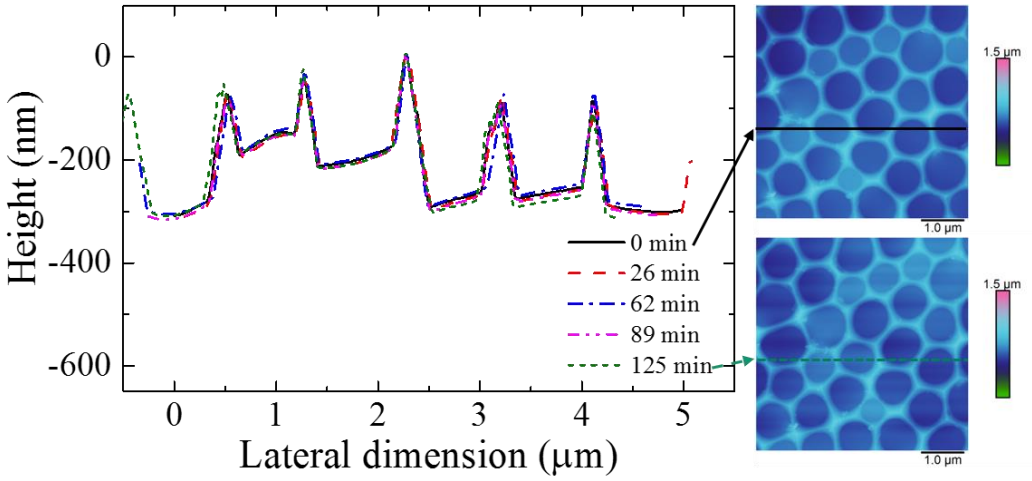

Figure S2. Evolution of cross-sectional profiles of a scan line on the underwater nanoporous surface with $D \approx 653$ nm together with the first and last topographic images.

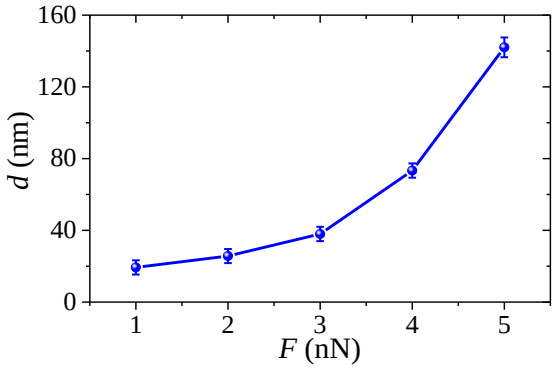

Figure S3. Water penetration depth d versus the scanning force F extracted from **Figure 4b** in the main text.

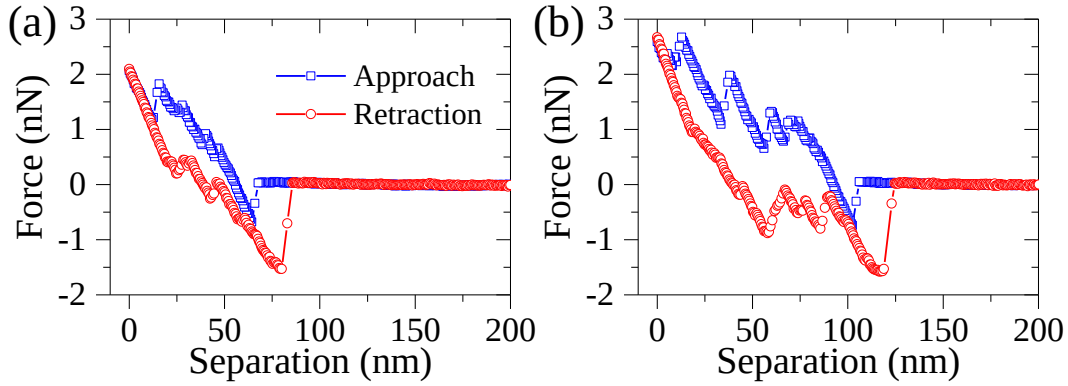

Figure S4. Representative *in situ* force curves acquired at indenting forces of 2 nN (**a**) and 3 nN (**b**) on the same nanomeniscus showed in **Figure 5a**.

Experimental parameters

Supplementary data S1:

In situ AFM images were captured at different times (see file names) on the nanoporous surface with $D \approx 362\,nm$ after the water droplet was deposited.

Probe: SNL-A; Scan size: 3μm; Scan rate: 1Hz; Peak Force Amplitude: 100nm; Peak Force Frequency: 2kHz; Peak Force setpoint: 1nN.

Supplementary data S2:

In situ AFM images captured at different scanning forces (see file names) on the nanoporous surface with $D \approx 362\,nm$ underneath the water droplet.

Probe: SNL-A; Scan size: 3μm; Scan rate: 1Hz; Peak Force Amplitude: 100nm; Peak Force Frequency: 2kHz.

Supplementary data S3:

Force curves acquired at different indenting forces on the nanoporous surface with $D \approx 653\,nm$ underneath the water droplet.

Probe: SNL-A; Ramp rate: 1Hz; Ramp Size: 500nm.

No.0-29: indenting force 1nN (0-26 on meniscus center, 27-29 on alumina part).

No.30-59: indenting force 2nN (30-56 on meniscus center, 57-59 on alumina part).

No.60-89: indenting force 3nN (60-86 on meniscus center, 87-89 on alumina part).